



OPEN 1'-O-methyl-averantin isolated from the endolichenic fungus *Jackrogersella* sp. EL001672 suppresses colorectal cancer stemness via sonic Hedgehog and Notch signaling

Mücahit Varlı¹, Eun-Young Lee², Yi Yang¹, Rui Zhou¹, İsa Taş¹, Sultan Pulat¹, Chathurika D. B. Gamage¹, So-Yeon Park¹, Jae-Seoun Hur³, Sang-Jip Nam^{2✉} & Hangun Kim^{1✉}

Endolichenic fungi are host organisms that live on lichens and produce a wide variety of secondary metabolites. Colorectal cancer stem cells are capable of self-renewal and differentiation into cancer cells, which makes cancers difficult to eradicate. New alternative therapeutics are needed to inhibit the growth of tumor stem cells. This study examined the ability of an extract of *Jackrogersella* sp. EL001672 (derived from the lichen *Cetraria* sp.) and the isolated compound 1'-O-methyl-averantin to inhibit development of cancer stemness. The endolichenic fungus *Jackrogersella* sp. EL001672 (KACC 83021BP), derived from *Cetraria* sp., was grown in culture medium. The culture broth was extracted with acetone to obtain a crude extract. Column chromatography and reverse-phase HPLC were used to isolate an active compound. The anticancer activity of the extract and the isolated compound was evaluated by qRT-PCR and western blotting, and in cell viability, spheroid formation, and reporter assays. The acetone extract of EL001672 did not affect cell viability. However, 1'-O-methyl-averantin showed cytotoxic effects against cancer cell lines at 50 µg/mL and 25 µg/mL. Both the crude extract and 1'-O-methyl-averantin suppressed spheroid formation in CRC cell lines, and downregulated expression of stemness markers ALDH1, CD44, CD133, Lgr-5, Msi-1, and EphB1. To further characterize the mechanism underlying anti-stemness activity, we examined sonic Hedgehog and Notch signaling. The results showed that the crude extract and the 1'-O-methyl-averantin inhibited Gli1, Gli2, SMO, Bmi-1, Notch-1, Hes-1, and the CSL complex. Consequently, an acetone extract and 1'-O-methyl-averantin isolated from EL001672 suppresses colorectal cancer stemness by regulating the sonic Hedgehog and Notch signaling pathways.

Abbreviations

ALDH1	Aldehyde dehydrogenase 1 family
CSC	Cancer stem cell
CD133	Cluster of differentiation 133
DMSO	Dimethyl sulfoxide
EPHB1	Ephrin type-B receptor 1
Lgr-5	G-protein coupled receptor-5
SMO	G-protein-coupled receptor smoothened
Gli	Gli family zinc finger

¹College of Pharmacy, Suncheon National University, 255 Jungang-ro, Suncheon, Jeonnam 57922, Republic of Korea. ²Department of Chemistry and Nanoscience, Ewha Womans University, Seoul 03760, Republic of Korea. ³Korean Lichen Res. Institute, Suncheon National University, 255 Jungang-ro, Suncheon, Jeonnam 57922, Republic of Korea. ✉email: sjnam@ewha.ac.kr; hangunkim@suncheon.ac.kr

HES	Hairy and enhancer of split
ITS	Internal transcribed spacer
NMR	Nuclear magnetic resonance
PTCH1	Protein patched homolog 1
PDA	Potato dextrose agar
PDB	Potato dextrose broth
SHH	Sonic Hedgehog

Cancer stemness cells are known for their potential for self-renewal and their ability to initiate growth of heterogeneous cancer cells¹. Increasing evidence shows that cancer stem cells (CSCs) contribute to chemoresistance^{2,3}, which limits the efficacy of anticancer drugs⁴. CSCs are found in many different types of cancer, including brain, kidney, breast, blood, lung, pancreatic, prostate, and colon cancers^{5,6}. Colon cancer is the second largest cause of cancer-related death, and the third most common cancer in the world in all sexes⁷. Although many therapeutic agents have been developed for the treatment of colon cancer, many treatments fail⁴. Therefore, it is important to prevent colon tumor formation and to search for new therapeutics that target CSCs.

Targeting CSCs primarily aims to block expression of stemness markers and embryonic signaling pathways (i.e., the sonic Hedgehog (SHH) and Notch pathways). CSCs express cluster of differentiation 133 (CD133), CD44, leucine-rich repeat-containing G protein-coupled receptor-5 (Lgr-5), and ephrin type-B receptor 1 (EPHB1)⁸, which are stem cell surface markers. In addition, ALDH1 is a stemness marker, overexpression of which correlates with development of CSCs⁹, and Musashi-1 promotes chemoresistance and cancer stemness in colorectal cancers¹⁰.

SHH is an important regulator of organogenesis during embryonic development¹¹. SHH ligands cause degradation of PTCH1, which activates of the G-protein-coupled receptors Smoothed (SMO) and Gli Family Zinc Finger 2 (Gli2)^{12,13}. In addition, inhibition of SMO regulates cell migration and cellular plasticity¹⁴. When acting as a transcription factor, Gli1 amplifies Hh signaling and so plays a key role in Hh signaling activity^{15–17}. In another pathway, called the stem cell signaling pathway, Notch plays a role in critical processes such as breast development, normal hematopoiesis, and maturation of the colorectal epithelium^{18,19}. Notch ligands are divided into two structurally separate groups, the Delta-like ligands (Dlls 1, 3, and 4) and the Jagged ligands (1 and 2), which bind to four transmembrane notch receptors²⁰. Thus, targeted suppression of stem cell formation in colorectal cancer (and other malignancies), chemoresistance, and relapse requires specific interventions that target relevant pathways.

Lichens produce nearly 1050 specific secondary metabolites that have antimicrobial, antiviral, antioxidant, antiallergic, and antitumoral effects^{3,21–27}. The Lichen thallus includes symbiotic endolichenic fungi within its structure. Endolichenic fungi species are thought to play an important ecological role by stimulating lichen formation and development, and by producing bioactive substances^{28–32}. Here, we examined the ability of the known metabolite 1'-O-methyl-averantin^{33,34}, isolated from a crude extract of the endolichenic fungus *Jackrogersella* sp. EL001672, to inhibit development of CSCs.

To the best of our knowledge, this is the first study to evaluate the anti-CSC potential of secondary metabolites of 1'-O-methyl-averantin from endolichenic fungus *Jackrogersella* sp.

Results

Identification of active compound from an EL001672 crude extract. Bioactivity-guided fractionation of a crude extract from EL001672 led to isolation of compound 1'-O-methyl-averantin (Fig. 1A,B, Supple Figs. 1–3). Previous studies suggest that 1'-O-methyl-averantin inhibits protein tyrosine phosphates and has weak antioxidant activity^{33,35}.

1'-O-methyl-averantin suppresses cancer stemness. MTT assays were performed to investigate the effect of the crude extract and 1'-O-methyl-averantin on the viability of colon cancer cell lines CSC221, Caco2, DLD1, and HCT116 for 48 h. The EL001672 crude extract had no significant effect on cell viability; however, 1'-O-methyl-averantin exerted cytotoxic effects against all cell lines at 50 µg/mL and 25 µg/mL. The IC₅₀ of 1'-O-methyl-averantin was 19.34 µg/mL in CSC221, 18.35 µg/mL in CaCo2, 21.502 µg/mL in DLD1, and 22.78 µg/mL in HCT116 (Fig. 1C,D). The doubling times of CaCo2, HCT116, and DLD1 cell lines are approximately 62 h, 22 h³⁶, 22 h³⁷, respectively. Here, 1'-O-methyl-averantin has cytotoxic effects in cell lines with different doubling times and may be a potential apoptosis-inducing agent. To further characterize whether 1'-O-methyl-averantin has selective cytotoxicity on CRC cells, it needs to test on non-transformed cells. The results tested in HEK293T (human embryonic kidney cells) cells showed that 1'-O-methyl-averantin also showed cytotoxic effect at 50 and 25 µg/ml (Supple Fig. 4). These results suggested that further investigations are required to verify the general cytotoxicity of 1'-O-methyl-averantin at high concentration. Potential future studies include extensive cytotoxic studies of 1'-O-methyl-averantin in different normal and cancer cell lines, as well as research ideas to achieve cancer-specific delivery and/or target-based optimization of the compound to maximize the efficacy and lower the toxicity.

1'-O-methyl-averantin inhibits spheroid formation in CRC cells. To confirm the concentration-dependent inhibitory effect of 1'-O-methyl-averantin and the crude extract on CSC activity in colorectal cancer cell lines, we evaluated spheroid formation by CSC221, DLD1, and HCT116 cells. Both the crude extract and 1'-O-methyl-averantin suppressed spheroid formation significantly, suggesting that the EL001672 crude extract and 1'-O-methyl-averantin inhibit cancer stemness (Fig. 2A–C).

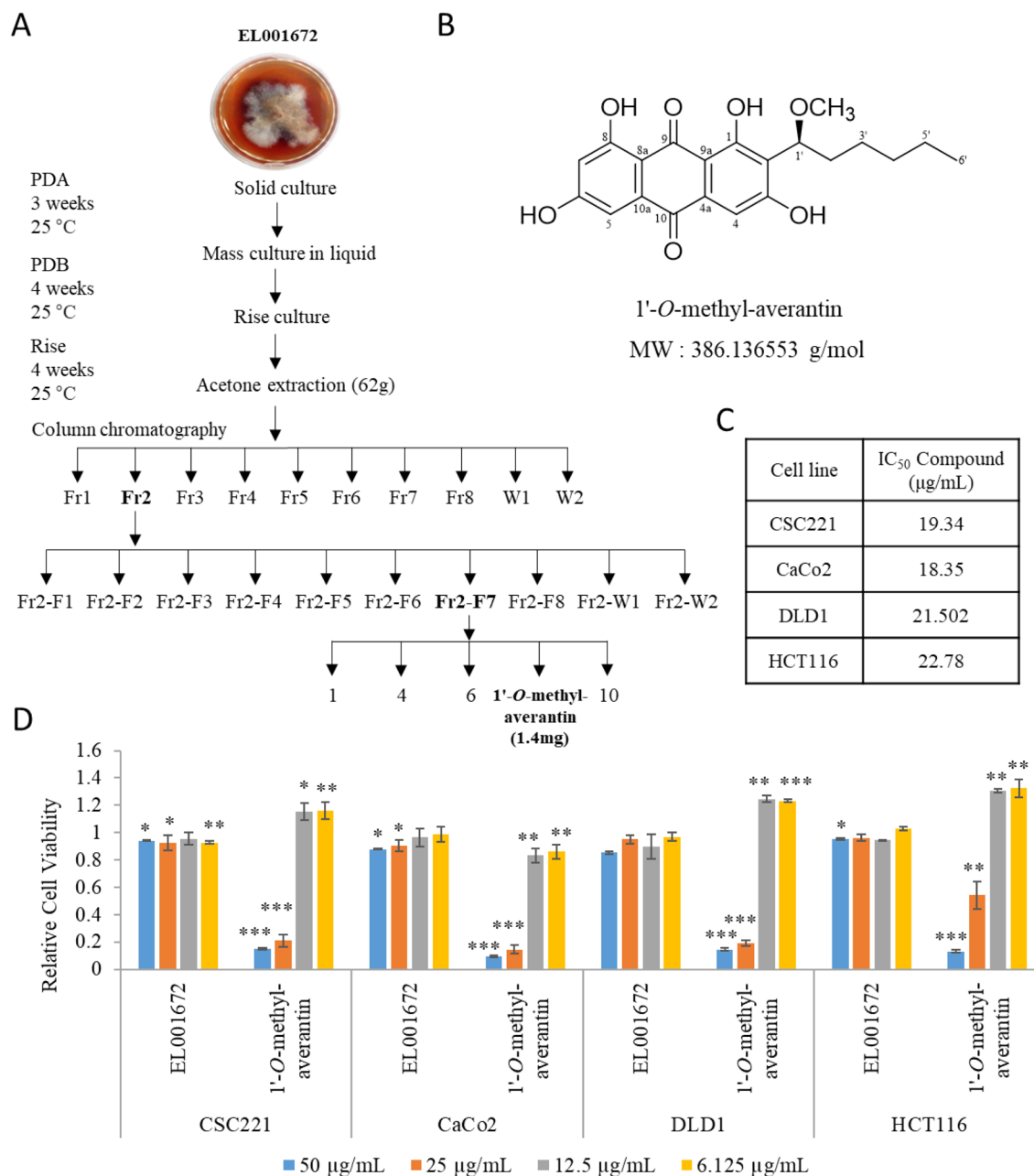


Figure 1. 1'-O-methyl-averantin, isolated from a crude extract of EL001672, suppresses cancer stemness. **(A)** Images of the endolichenic fungus EL001672 isolated from *Cetraria* sp., and a flow chart illustrating isolation of the pure compound 1'-O-methyl-averantin. **(B)** Chemical structure of 1'-O-methyl-averantin. **(C)** IC₅₀ values of 1'-O-methyl-averantin against the CSC221, CaCo2, DLD1, and HCT116 cell lines. **(D)** Viability of cancer cell lines treated with EL001672 crude extract and 1'-O-methyl-averantin. DMSO used as a control. 50, 25, 12.5 and 6.125 µg/ml 1'-O-methyl-averantin represent a concentration of 129.49, 64.74, 32.37 and 16.19 µM, respectively. Data represent the mean ± standard error of the mean, *p < 0.05; **p < 0.01; ***p < 0.001 (compared with DMSO-treated cells).

1'-O-methyl-averantin suppresses expression of CSC markers. To examine whether the crude extract and 1'-O-methyl-averantin inhibit expression of cancer stemness markers in CSC221 cells, we measured expression of mRNA encoding ALDH1, CD133, CD44, Lgr5, Msi-1, and EphB1 (Fig. 3A,B). Both the crude extract and 1'-O-methyl-averantin downregulated expression of cancer stemness markers in a dose-dependent manner. However, immunoblot analysis suggested downregulation of ALDH1, CD44, CD133, Lgr-5, and Msi-1 protein expression (Fig. 3C–F).

1'-O-methyl-averantin inhibits the SHH signaling pathway in CSC221 cells. Next, we examined expression of the SHH pathway genes and proteins, and conducted reporter assays to examine the pathways inhibited by 1'-O-methyl-averantin. Changes in the expression of SHH pathways mRNA levels were observed

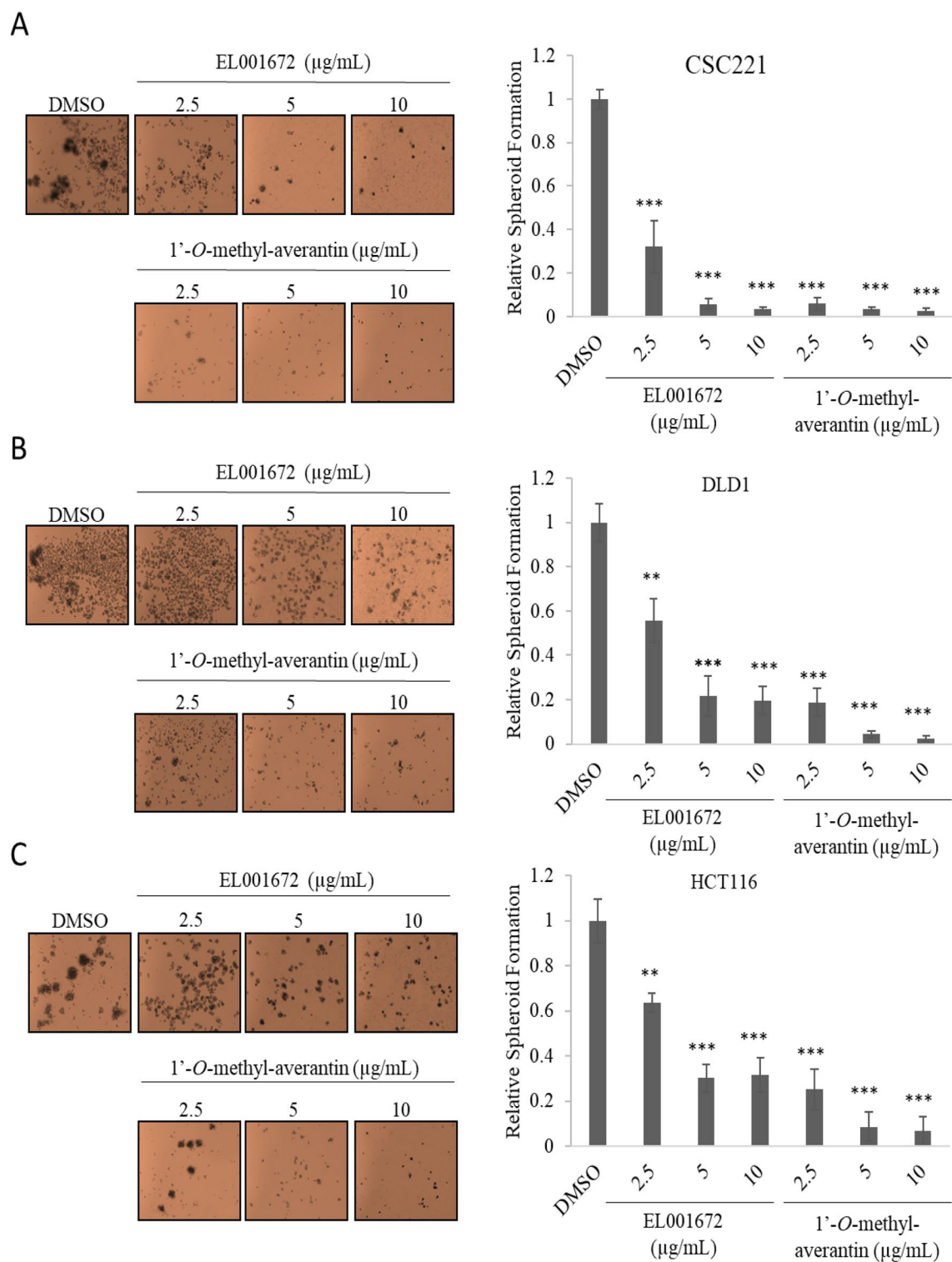


Figure 2. EL001672 extract and 1'-*O*-methyl-averantin inhibit colorectal cancer cell stemness. (A–C) Representative images of spheroid formation by CSC221, DLD1, and HCT116 cells treated with EL001672 extract or 1'-*O*-methyl-averantin for 14 days, and quantitative analysis of the number of spheroids formed following each treatment. 10, 5 and 2.5 µg/ml 1'-*O*-methyl-averantin represent a concentration of 25.90, 12.95 and 6.47 µM, respectively. Data represent the mean ± standard error of the mean, **p* < 0.05; ***p* < 0.01; ****p* < 0.001.

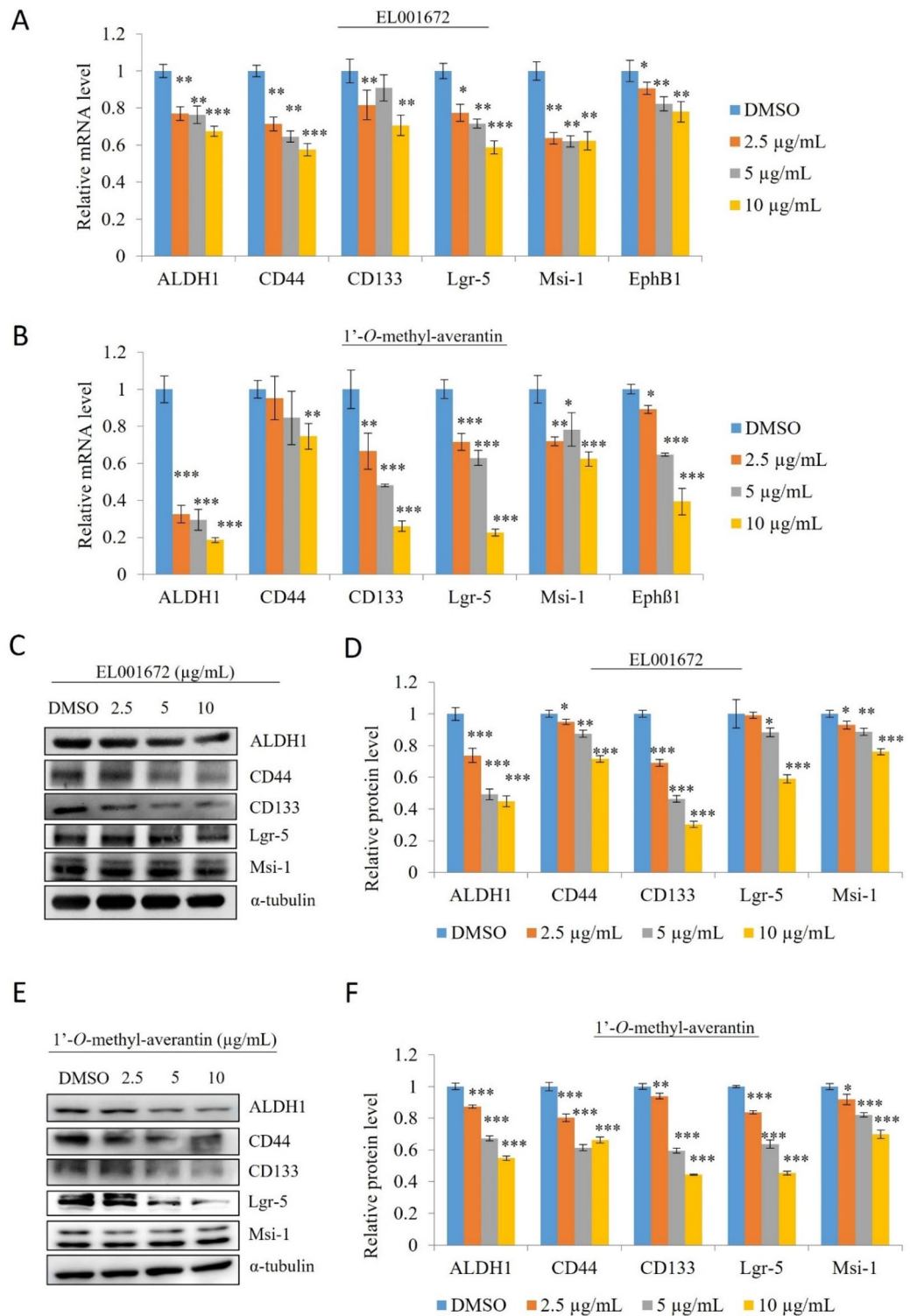


Figure 3. A crude extract of EL001672 and 1'-O-methyl-averantin suppress expression of cancer stemness markers. CSC221 cells were treated for 48 h with a crude extract of EL001672 or 1'-O-methyl-averantin for mRNA and protein expressions. (A,B) Quantitative analysis of mRNA encoding cancer stem markers aldehyde dehydrogenase-1 (ALDH1), cluster of differentiation 133 (CD133), CD44, Lgr5, Musashi-1, and EphB1. CSC221 cells were treated for 48 h with a crude extract of EL001672 or 1'-O-methyl-averantin. (C,E) Immunoblots are shown. Relative expression of each target protein after cells were exposed to a crude extract of EL001672 (D) or 1'-O-methyl-averantin (F). 10, 5 and 2.5 µg/ml 1'-O-methyl-averantin represent a concentration of 25.90, 12.95 and 6.47 µM, respectively. Data represent the mean ± SEM. *p < 0.05; **p < 0.01 (compared with DMSO-treated CSC221 cells).

in CSC221 cells treated with the crude extract or 1'-O-methyl-averantin. As shown in Fig. 4A and D, expression of Gli1, Gli2, SMO, and Bmi-1 mRNA was downregulated significantly, and in a dose-response manner. Western blot analysis revealed significant downregulation of Gli1, Gli2, SMO, and Bmi-1 protein expression in CSC221 cells (Fig. 4B,C,E,F). Next, we used NIH3T3 cells harboring an integrated Gli reporter gene to examine Gli luciferase activity in the presence of the crude extract, 1'-O-methyl-averantin, GANT61 (a Gli inhibitor), and Vismodegib (a SMO inhibitor). 1'-O-methyl-averantin suppressed Gli activity significantly at all concentrations tested, with an effect similar to that of the Gli inhibitor (Fig. 5A). Then, we designed Gli-expressed cell models to further characterize how the SHH signaling pathway regulates the upstream flow. 1'-O-methyl-averantin suppressed luciferase activity in HEK293T cells, similar to the results of the reporter assay in NIH3T3-Gli-luc cells. Groups of the cell with Gli-luc, Gli1-mediated Gli-luc and Gli2-mediated Gli-luc were silenced with an SMO-specific si-RNA. Silencing SMO downregulated Gli-luc activity compared to the negative control group, and 1'-O-methyl-averantin retained its Gli inhibition ability in the group of cells with si-SMO. Cells overexpressing Gli1 and/or Gli2 restored si-SMO mediated downregulation in Gli-luc activity and compound treatment in this cell successfully downregulated Gli1- and/or Gli2-induced Gli-luc activity. Particularly, 1'-O-methyl-

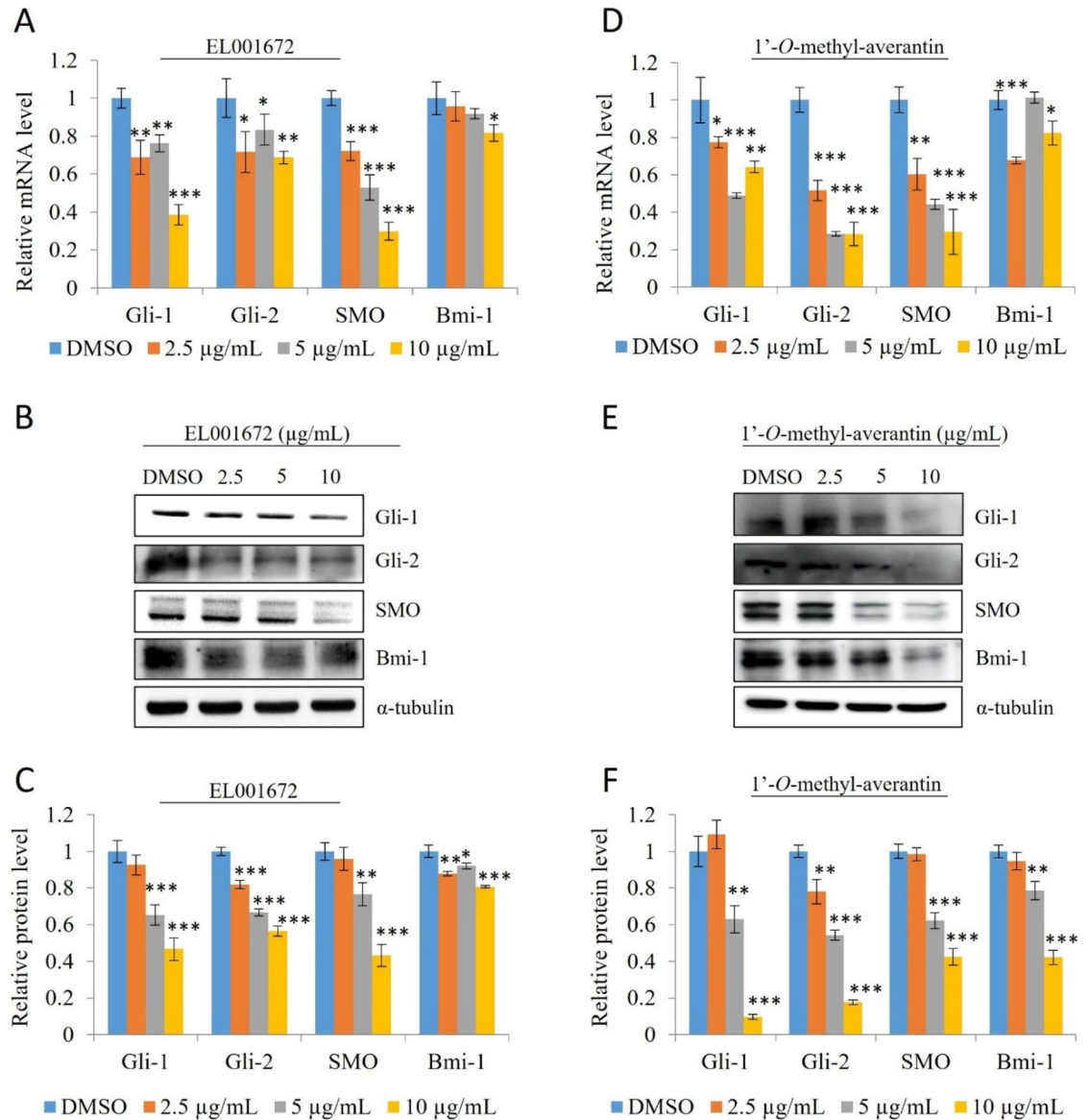


Figure 4. The crude extract of EL001672 and 1'-O-methyl-averantin block the sonic Hedgehog (SHH) signaling pathway. (A,D) Expression of mRNA encoding Gli1, Gli2, SMO, and Bmi-1 by CSC221 cells after treatment with the indicated concentrations of crude extract or 1'-O-methyl-averantin and incubated 48 h. (B–E) Western blot analysis of Gli1, Gli2, SMO, and Bmi-1 protein levels in CSC221 cells treated with indicated concentrations of crude extract and 1'-O-methyl-averantin and incubated 48 h. (C–F) Quantitative analysis of protein expression. 10, 5 and 2.5 µg/ml 1'-O-methyl averantin represent a concentration of 25.90, 12.95 and 6.47 µM, respectively. Data represent the mean \pm standard error of the mean, * $p < 0.05$; ** $p < 0.01$; *** $p < 0.001$; difference compared with DMSO-treated.

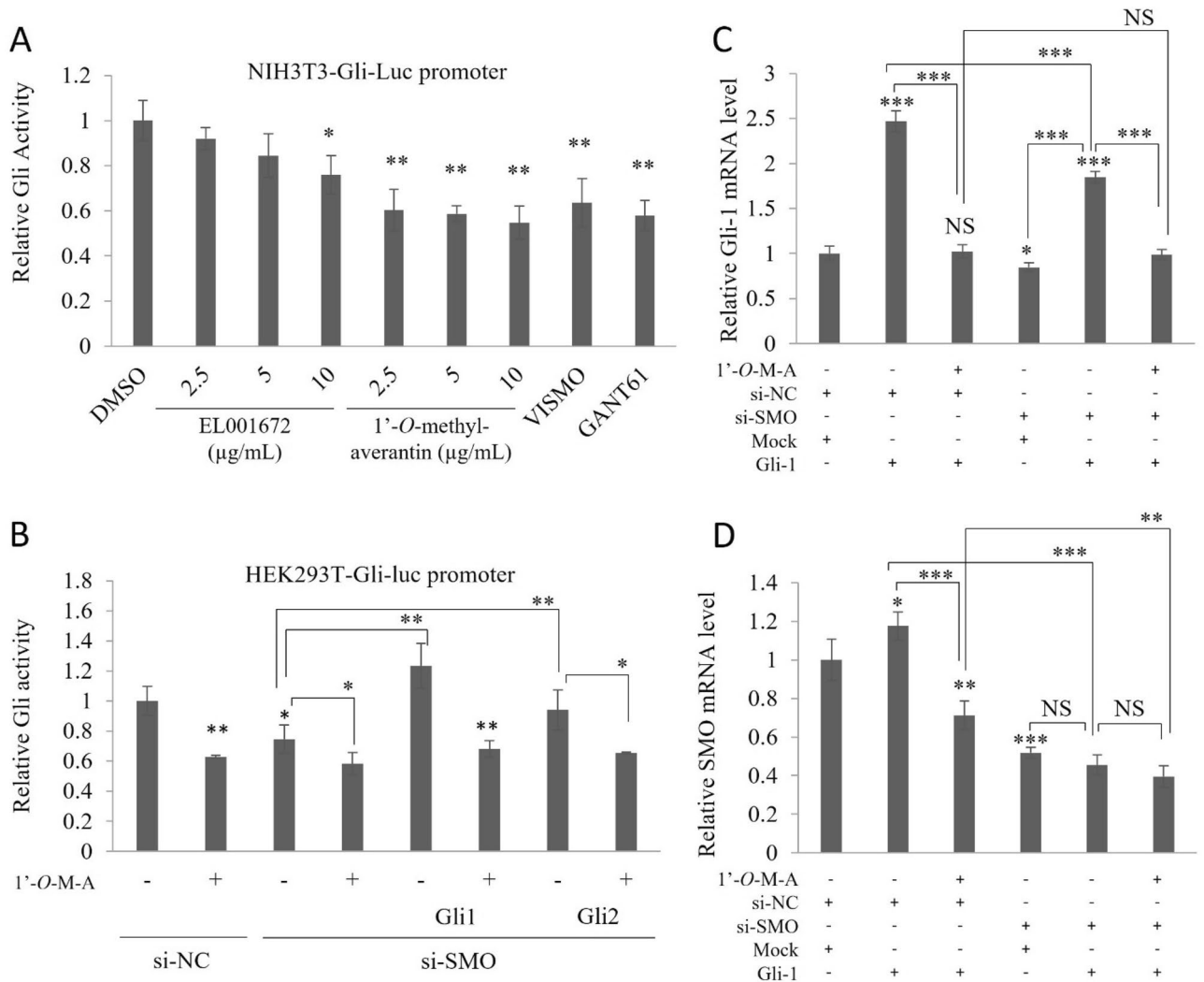


Figure 5. Inhibitory effect of 1'-O-methyl-averantin on Gli-overexpression models. **(A)** Gli-luc reporter assays: NIH 3T3 cells stably incorporating Gli-dependent firefly luciferase and constitutive Renilla luciferase reporters were treated with 2.5, 5 or 10 µg/mL crude extract, 1'-O-methyl-averantin, 5 µg/mL GANT61 (a Gli inhibitor), and Vismodegib-GDC-0449 (a SMO inhibitor) and incubated 48 h. **(B)** Gli-luc reporter assays in HEK293T. HEK293T cells transfected with si-negative control and/or si-SMO for 12 h, and then cells were exposed to Gli-luc plasmid and Gli1 or Gli2 plasmid transfection for 12 h. After that cell treated with DMSO or 1'-O-methyl-averantin for 48 h. **(C,D)** Quantitative analysis of mRNA expression levels of Gli1 and SMO on HEK293T cells. HEK293T cells transfected with si-negative control and/or si-SMO for 12 h, and then cells were exposed to Gli1 plasmid and/or mock transfection for 12 h. After that cell treated with DMSO or 1'-O-methyl-averantin for 48 h. 10, 5 and 2.5 µg/ml 1'-O-methyl-averantin represent a concentration of 25.90, 12.95 and 6.47 µM, respectively. Data represent the mean ± standard error of the mean, * $p < 0.05$; ** $p < 0.01$; *** $p < 0.001$; difference compared with DMSO-treated.

averantin more dramatically suppresses Gli1-induced Gli-luc activity (Fig. 5B). For further validation, we checked the levels of Gli1 and SMO mRNA by qRT-PCR in cells overexpressed Gli1 and subsequently in cells in which SMO was silenced. 1'-O-methyl-averantin treatment dramatically suppressed Gli1 mRNA levels in Gli1-induced and SMO-silenced or non-silenced cell groups. In addition, there was no statistically significant difference between the inhibition activities of Gli-1 mRNA expression of the SMO-silenced compound treatment group and the non-silenced compound treatment groups. Our results show that inhibition of the SHH signaling pathway downstream effector Gli1 occurs independently of the upstream receptor SMO (Fig. 5C,D). Taken together, these results suggest that the SHH signaling pathway plays a major role in inhibition of colorectal cancer stemness by 1'-O-methyl-averantin.

1'-O-methyl-averantin suppresses the Notch signaling pathway in CSC221 cells. Next, we evaluated the potential inhibitory effect of the crude extract and 1'-O-methyl-averantin on the Notch signaling pathway in CSC221 cells. We used quantitative RT-PCR to measure expression of Notch-1 and Hes-1 mRNA. The results showed that expression of both Notch-1 and Hes-1 mRNA was downregulated significantly by the crude extract.

1'-O-methyl-averantin tended to downregulate expression of Notch-1 and Hes-1 mRNA at all concentrations tested, but showed statistically significant levels of inhibition at concentrations of 5 and 10 $\mu\text{g}/\text{mL}$ (Fig. 6A,B). Next, we used HEK293T-transfected cells to conduct a dual luciferase promoter assay to examine suppression of Hes-1 (hairy and enhancer of split-1)-luc and CSL (CBF1/Su(H)/Lag-1)-luc promoter activity (Fig. 6C,D). Crosstalk between the SHH and Notch signaling pathways mean that these pathways can regulate each other³⁸. Therefore, we compared the inhibitory activity of Gli and SMO inhibitors with that of the crude extract and 1'-O-methyl-averantin. The crude extract and 1'-O-methyl-averantin significantly downregulated Hes-1-luc and CSL-luc promoter activity to levels observed for the Gli and SMO inhibitors.

Discussion

Many compounds of lichen origin have effects on tumor progression, cell cycle progression, apoptosis, angiogenesis, energy metabolism, and immune modulation^{39–42}. In this study, we isolated 1'-O-methyl-averantin from an endolichenic fungi acetonic extract of *Cetraria* sp. Previous studies show that an unidentified marine-derived fungus ZSUH-36 isolated from *Acanthus ilicifolius* Linn., and the marine-derived fungus *Aspergillus* sp. SCSIO F063, produce 1'-O-methyl-averantin^{34,43}. 1'-O-methyl-averantin has structural similarities with many compounds and is classified as an anthraquinone⁴⁴. Anthraquinone derivatives have antitumor activity and cytotoxic activity, as well as effects on the cell cycle and apoptosis^{45–49}. However, no study has examined the anticancer activity of 1'-O-methyl-averantin in detail. Here, we evaluated the effect of a crude extract of EL001672, as well as 1'-O-methyl-averantin, on colorectal cancer cells. Several colorectal cancer cell lines were used in this study. DLD1 has mutant KRAS, BRAF, PIK3CA, TP53, and APC and MSI; Caco2 has wild-type KRAS, BRAF, PIK3CA, TP53, APC and MSS; HCT116 has KRAS mutant; CSC221 is human colorectal adenocarcinoma-enriched cancer stem cell^{50,51}. The results were as follows: (1) 1'-O-methyl-averantin was cytotoxic to CSC221, CaCo2, DLD1, and HCT116 cells; (2) 1'-O-methyl-averantin and the crude extract suppressed spheroid formation by colorectal cancer cells; (3) 1'-O-methyl-averantin and the crude extract downregulated expression of cancer stem cell markers; (4) 1'-O-methyl-averantin and the crude extract inhibited the SHH signaling pathway was markedly inhibited with 1'-O-methyl-averantin in CSCs cell; and (5) 1'-O-methyl-averantin and the crude extract inhibited

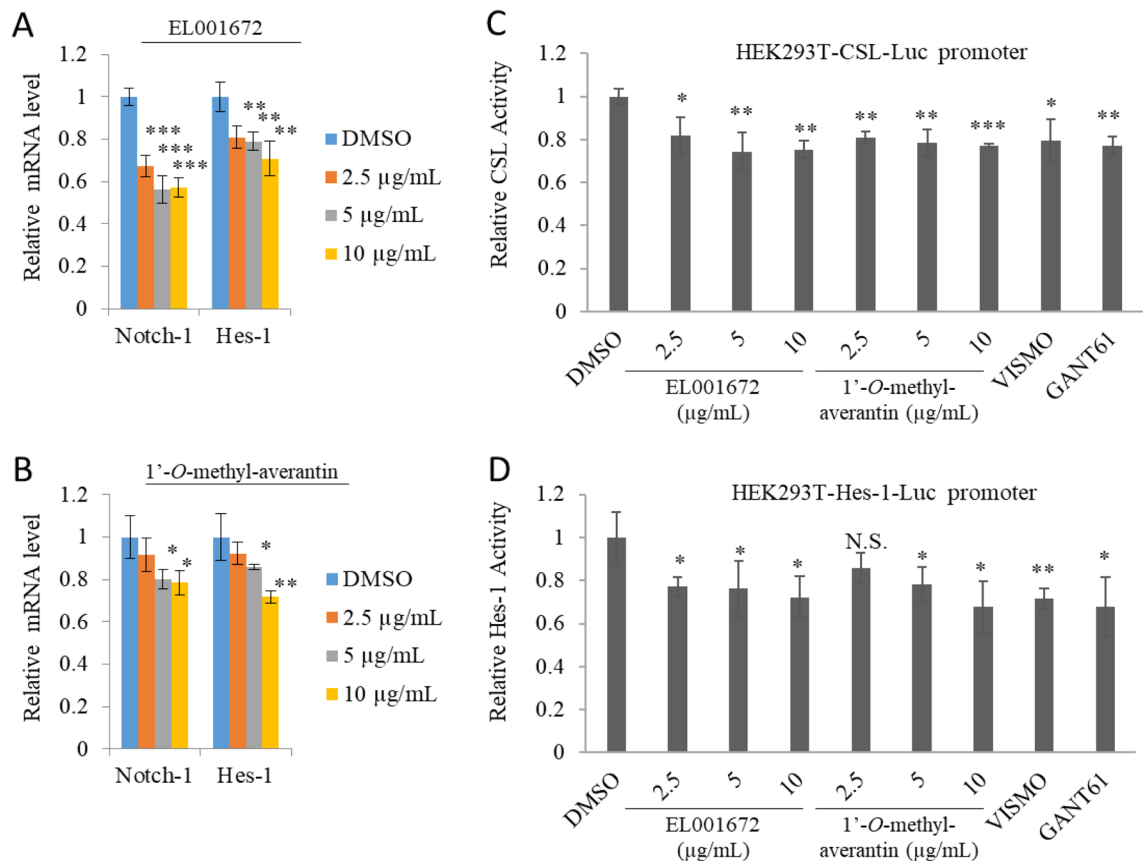


Figure 6. Effect of a crude extract of EL001672 and 1'-O-methyl-averantin on the NOTCH signaling pathway. (A,B) Quantitative analysis of Notch-1 and Hes-1 (hairy and enhancer of split-1) mRNA expression by CSC221 cells treated with the indicated concentrations of crude extract or 1'-O-methyl-averantin and incubated 48 h. (C,D) CSL (CBF1/Su(H)/Lag-1)-luc and Hes-1 reporter assays in HEK293T cells treated with 2.5, 5, or 10 $\mu\text{g}/\text{mL}$ crude extract, 1'-O-methyl-averantin, 5 $\mu\text{g}/\text{mL}$ GANT61 (a Gli inhibitor), and Vismodegib-GDC-0449 (a SMO inhibitor) and incubated 48 h. 10, 5 and 2.5 $\mu\text{g}/\text{mL}$ 1'-O-methyl-averantin represent a concentration of 25.90, 12.95 and 6.47 μM , respectively. Data represent the mean \pm standard error of the mean. * $p < 0.05$; ** $p < 0.01$; *** $p < 0.001$; difference compared with each groups.

Notch signaling at the transcriptional level. Collectively, the data show that 1'-*O*-methyl-averantin suppresses colorectal cancer stemness by regulating the SHH and Notch signaling pathways, suggesting that it may have potential as a therapeutic drug.

CSCs drive cancer formation and metastasis. Therefore, developing treatment modalities that target CSCs has great potential^{52,53}. The SHH and Notch signaling pathways play major roles in cancer development, and so are themselves a possible therapeutic target^{54,55}. The transmembrane response to the SHH ligand is modulated and mediated by two transmembrane proteins: PTCH and SMO. Gli1 and Gli2 are downstream targets of SHH signaling⁵⁶. In this study, we measured expression of SMO, Gli1, and Gli2 mRNA and protein, and found that both were inhibited by 1'-*O*-methyl-averantin and the crude extract. Moreover, 1'-*O*-methyl-averantin and crude extract inhibited Gli reporter activity in stable Gli-overexpressing cells. The inhibitory activity of 1'-*O*-methyl-averantin at 2.5, 5, and 10 µg/mL was similar to that of a Gli inhibitor (GANT61) and an SMO inhibitor (Vismodegib) used at 5 µg/mL. On the other hand, the crude extract can significantly suppress Gli reporter activity at a concentration of 10 µg/ml, but has a weaker inhibitory effect than 1'-*O*-methyl-averantin. The anti-stemness activity of 1'-*O*-methyl-averantin was suppressed the SHH pathway, with SMO, Gli1, and Gli2. Moreover, 1'-*O*-methyl-averantin targets the SHH signaling pathway via Gli1, independently of SMO. SHH signaling increases Bmi-1 expression, which in turn drives cellular reprogramming^{57,58}. In particular, the downstream transcription factor Gli within the SHH pathway induces expression of Bmi-1⁵⁹⁻⁶¹. Our results suggest that after treatment 1'-*O*-methyl-averantin and crude extract, Bmi-1 expression tended to be downregulated.

Studies reported that crosstalk between the SHH and Notch signaling pathways results in them regulating each other⁶²⁻⁶⁴. Therefore, we examined the effects of the pure compound and crude extract on Notch signaling. When notch ligands bind to Notch receptors, γ -secretase liberates the intracellular domains of the NICD (Notch receptor) via proteolytic cleavage (S3 cleavage). The NICD undergoes nuclear translocation and associates with the transcription factor CSL. The NICD/CSL complex activates Hes1 and other Notch signaling target genes⁶⁵⁻⁶⁷. Here, we used qRT-PCR and a reporter assay to evaluate inhibition of Notch signaling by 1'-*O*-methyl-averantin and the crude extract. The results showed that Notch-1 and Hes-1 mRNA tended to be downregulated after treatment. In addition, CSL and Hes-1 reporter activity were inhibited by both the crude extract and 1'-*O*-methyl-averantin.

ALDH1, CD133, CD44, Lgr5, Msi-1, and EphB1 are markers of cancer stemness^{3,8,68,69}. Human colon tumors are characterized by CD133+CD44+ cells, which are known as CSCs or tumor-starting cells^{70,71}. The G-protein-coupled receptor family of proteins includes the leucine-rich repeat-containing G protein-coupled receptor 5 (Lgr5), also known as GPR49. Lgr5 is a target of Wnt signaling, and a selective and ideal cancer stem cell marker^{72,73}. EphB receptors coordinate proliferation and migration within the intestinal stem cell niche⁷⁴⁻⁷⁶. Our data suggest that 1'-*O*-methyl-averantin downregulates expression of multiple stem cell markers associated with colorectal cancer.

ALDH1 levels are associated with liver metastases, tumor progression, drug resistance, and a poor clinical outcome^{77,78}. Studies suggest that deletion of Gli-1 reduces expression of ALDH1 and CD44⁷⁹, and that ALDH1 can modulate expression of Gli⁸⁰. The novel inhibitors GANT61 (inhibitor of Gli1 and Gli2 targeting the Hedgehog/GLI pathway) and DAPT (inhibitor of Notch, a γ -secretase substrate) downregulate ALDH1 expression^{81,82}. Our results show that 1'-*O*-methyl-averantin significantly downregulated expression of ALDH1 at both the mRNA and protein levels. Previous studies tried to identify the mechanism underlying the links between ALDH1-SHH and ALDH1-Notch⁸²⁻⁸⁸, the data presented in the present study suggest that 1'-*O*-methyl-averantin and the crude extract have co-inhibitory effects on ALDH1, SHH, and Notch signaling.

Materials and methods

General experimental procedures. NMR spectra were acquired by containing Me₄Si as internal standard on Varian Inova spectrometers 400 MHz and 100 MHz spectrometer (Varian Medical Systems, Inc., Virginia, USA) using solvent DMSO-*d*₆ (Cambridge Isotope Laboratories (CIL), Inc., Tewksbury, MA, USA). Low-resolution LC-MS measurements were performed using the Agilent Technology 1260 quadrupole (Agilent Technologies, Santa Clara, CA, USA) and Waters Alliance Micromass ZQ LC-MS system (Waters Corp, Milford, MA, USA) using reversed-phase column (Phenomenex Luna C18 (2) 100 Å, 50 mm × 4.6 mm, 5 µm) (Phenomenex, Torrance, CA, USA) at a flow rate 1.0 mL/min at the National Research Facilities and Equipment Center (NanoBioEnergy Materials Center) at Ewha Womans University. Optical rotations were acquired using a Kruss Optronic P-8000 polarimeter with a 5-cm cell (Kruss, Habrug, Germany).

The compound is an orange-red amorphous powder. LR-ESI-MS spectroscopic data revealed an ionic peak at *m/z* 372.3 [M+H]⁺. The ¹H NMR spectrum of 1'-*O*-methyl-averantin displayed two meta-coupled aromatic protons [δ_{H} 7.10 (1H, d, *J* = 2.3 Hz, H-5), three hydroxyl groups [δ_{H} 12.82 (1H, s, 1-OH), δ_{H} 12.15 (1H, s, 8-OH), and δ_{H} 6.58 (1H, d, *J* = 2.3 Hz, H-7)], and one methoxy proton [δ_{H} 3.15 (3H, s, 1'-OCH₃)]. The ¹³C NMR spectrum of 1'-*O*-methyl-averantin revealed 12 carbons. HSQC spectra revealed two carbonyl carbons [δ_{C} 188.8 (C-9), and δ_{C} 181.4 (C-10)], a methoxy carbon [δ_{C} 56.3 (C-OCH₃)], nine fully-substituted carbons [δ_{C} 165.4 (C-8), δ_{C} 164.4 (C-1), δ_{C} 164.0 (C-6), δ_{C} 163.2 (C-3), δ_{C} 133.5 (C-10a), δ_{C} 134.9 (C-4a), δ_{C} 119.4 (C-2), δ_{C} 108.8 (C-8a), and δ_{C} 108.1 (C-9a)], four methylene carbons [δ_{C} 32.5 (C-2'), δ_{C} 31.2 (C-4'), δ_{C} 25.4 (C-3'), and δ_{C} 22.1 (C-5')], four methine carbons [δ_{C} 108.5 (C-5), δ_{C} 108.7 (C-4), δ_{C} 108.2 (C-7), and δ_{C} 74.6 (C-1')], and one methyl carbon [δ_{C} 13.9 (C-6')]. Based on a comparison with NMR data in the literature, the compound was identified as 1'-*O*-methyl-averantin^{89,90}. The NMR data are available in Supplementary Figs. 5–9. Optical rotation of **1** ($[\alpha]_{\text{D}}^{25}$ = +24.09°, *c* 0.11, CH₃OH) suggested that the absolute configuration at C-1' should be an (*R*)-configuration⁹⁰.

Fungal strain. Lichen specimen of *Cetraria* sp. was collected from the Yunnan, baima snow mountain. Voucher specimens were deposited in the Korean Lichen Research Institute, Suchon National University,

Korea (<https://cc.aris.re.kr/kolabic>). The endolichenic fungus EL001672 was isolated from the lichen specimen of *Cetraria* sp. using the surface sterilization method⁹¹.

As already shown, fungus internal transcribed spacer sequencing was carried out²⁵. DNA was extracted from EL001672 cultured on PDA using a DNeasy Plant Mini Kit following the manufacturer's protocols (Qiagen, Hilden, Germany). The internal transcribed spacer (ITS) region of the rDNA was amplified with the universal primers ITS1F (5'-CTTGGTCATTTAGAGGAAGTAA-3')⁹² and LR5 (5'-ATCCTGAGGGAACTTC-3')⁹³. EL001672, was determined as *Jackrogersella* sp. by the BLAST search of the ITS sequence, which showed 98.99% similarity to that of *Jackrogersella multififormis* (GenBank Accession No. ON453667.1). The ITS sequence of *Jackrogersella* sp. EL001672 is available in Supplementary Table 1.

Preparation of endolichenic fungal extracts. Firstly, EL001672 grew on potato dextrose agar (PDA) medium at 25 °C. Mycelial growth was monitored in 500 ml Erlenmeyer flasks containing 200 ml of potato dextrose broth (PDB) incubated at 25 °C on a rotary shaker at 150 rpm for 4 weeks. Next, EL001672 cultured in liquid culture was subjected to rice culture for 4 weeks. Separation of mycelium on the surface was achieved. The mycelia were dried and then extracted with acetone. To produce the crude extract (62 g), the organic phase was then evaporated to dryness under a vacuum. For use in additional investigations, the dried extracts were then completely dissolved in DMSO.

Isolation of active compound from EL001672. The crude extract of EL001672 (62 g) was fractionated by the flash column chromatography on silica gel eluted with CH₂Cl₂/CH₃OH (100/0, 100/2, 100/1, 100/5, 100/10, 100/20, 100/50, 100/100 and 0/100, v/v, each of 600 mL) to obtain eight fractions (Fraction 1 to Fraction 8). The fraction two (7.88 g) was further fractionated by the flash column chromatography on C-18 resin eluted with H₂O/CH₃OH (80/20, 60/40, 50/50, 40/60, 30/70, 20/80, 0/100, each of 600 mL) to obtain eight subfractions (Fraction 1 to Fraction 8). The subfraction seven was isolated by reversed-phase HPLC (Phenomenex Luna C-18 (2), 250 × 100 mm, 2.0 mL/min, 5 μm, 100 Å, UV = 280 nm) using an isocratic condition 85% CH₃CN in H₂O to obtain 1'-O-methyl-averantin (1.4 mg, t_R = 22.5 min).

Cell culture and Reagents. CSC221 (human colorectal adenocarcinoma-enriched CSCs), CaCo2 (MSS and wild-type KRAS, BRAF, and PIK3CA), DLD1 (MSI and mutant KRAS and PIK3CA), HT116 (KRAS mutation), HEK293T (human embryonic kidney cells) cells were used in this research. CSC221 cell was cultured in DMEM (GenDepot, Katy, TX, USA) supplemented with 10% fetal bovine serum (FBS) and 1% penicillin streptomycin solution. HEK293T, CaCo2, DLD1, and HCT116 cell lines were purchased from the American Type Culture Collection (ATCC, Manassas, VA, USA). CSC221 cell line was purchased from BioMedicure (San Diego, CA, USA). Cells were incubated in 5% CO₂ in a humidified atmosphere at 37 °C⁵¹. GANT61 (G9048) was purchased from Sigma-Aldrich and Vismodegib-GDC-0449 (A10258) was purchased from AdooQ Bioscience (Irvine, CA, USA).

MTT assay. Cells were seeded at a density of 2.5 × 10³ cells/well in 96-well plates, after overnight cells were treated with crude extract of EL001672 and 1'-O-methyl-averantin for 48 h incubation. The 3-(4,5-dimethylthiazol-2-yl)-2,5-diphenyltetrazolium bromide (MTT) was added and maintained for 4 h once treatment was completed. DMSO was added after removing the medium. Absorbance at 570 nm was determined using a microplate reader with Gen 5 (2.03.1) software (BioTek, Winooski, VT, USA)^{94,95}.

Spheroid assay. Cells were trypsinized at that point washed with N2-supplemented DMEM/F12 (Invitrogen, Carlsbad, CA, USA). Human basic fibroblast growth factor (hbFGF; 10 ng/mL; Invitrogen) and human recombinant epidermal growth factor (hrEGF; 20 ng/mL; Biovision, Atlanta, GA, USA) are added in N2-supplemented DMEM/F12⁹⁶. After CSC221 cells seeded at a density of 5 × 10³ cells/well in ultra-low attachment 24-well plates (Corning Inc., Corning, NY, USA). After 14 days of incubation, spheres were quantitated by inverted phase contrast microscopy. The relative sphere formation ability was calculated through the IMT iSolution software (IMT iSolution Inc., Northampton NJ, USA)⁹⁷ measuring the pixel intensity of the sphere area randomly in each plate. Data are presented as the average of three independent experiments.

Western blotting. CSC221, cells treated for 48 h were washed twice with ice-cold phosphate-buffered saline (PBS) and lysed in lysis buffer²⁴. Antibodies against ALDH1 (sc-166362; Santa Cruz Biotechnology, Dallas, TX, USA), CD133 (CA1217; Cell Applications, San Diego, CA, USA), CD44 (3570; Cell Signaling Technology, Danvers, MA, USA), Lgr-5 (ab75850; Abcam, Cambridge, MA, USA), Msi-1 (ab52865, Abcam), Gli1 (sc-20687; SANTA CRUZ, Dallas, TX, USA), Gli2 (sc-271786; SANTA CRUZ), Smoothered (SMO; ab72130; Abcam, Cambridge, MA, USA), Bmi-1 (ab38295; Abcam) were used to detection. α-tubulin (2125, Cell Signaling Technology) and β-Actin (sc-47778; SANTA CRUZ) antibody was used as an internal control. The bands were cut according to the protein size region of interest before incubating with antibodies and then imaged with an Immobilon Western Chemiluminescent HRP Substrate Kit (Merck Millipore, Billerica, MA, USA). Uncropped images of the blot images are presented as additional data (Supple Figs. 10, 11). Bands relative density was calculated based on the density of α-tubulin and actin bands in each sample. Values were demonstrated as arbitrary densitometric units corresponding to signal intensity.

Plasmids, si-RNA and reporter assay. SMO siRNA (human specific) and si-negative control purchased from Santa Cruz Biotechnology. The si-RNA and si-negative control were transfected by Lipofectamine RNAiMAX protocol. Gli1 and Gli2 plasmid was transfected into HEK293T cells using X-treme GENE 9 DNA.

NIH3T3-Gli-luc cells (stably incorporating Gli-dependent firefly luciferase and constitutive Renilla luciferase reporters) using for Gli reporter activity. HEK293T cells were transfected with Hes-1-, and CSL-conjugated firefly plasmid along with *Renilla-luc* (pRL-TK) plasmid using the X-treme GENE 9 DNA transfection reagent (Roche, Werk Penzberg, Germany). At 24 h after transfection, cells were treated with crude extract of EL001672 and 1'-*O*-methyl-averantin, or DMSO and incubated for 48 h at 37 °C under 5% CO₂. Normalized luciferase activity was obtained against Renilla activity to determine the transfection efficiency using a Dual-Luciferase reporter assay system (Promega, Madison, WI, USA)⁹⁸.

Quantitative reverse-transcription PCR (qRT-PCR). Quantitative RT-PCR (qRT-PCR) was conducted as already depicted³. Total RNA was isolated from CSC221 cells using RNAiso Plus (TaKaRa, Otsu, Japan). 1 mg of RNA was converted to cDNA using M-MLV reverse transcriptase (Invitrogen, Carlsbad, CA, USA). qPCR was performed using SYBR Green (Enzymomics, Seoul, Korea)⁹⁹. Primers for real-time PCR are listed in Supplementary Table 2. qRT-PCR reactions and analyses were performed on a CFX instrument (Bio-Rad, Hercules, CA, USA)¹⁰⁰.

Statistical analysis. All experiments were performed in triplicate. Data are expressed as means ± standard deviation. All statistical analyses were performed using the Sigma Plot software¹⁰¹.

Conclusion

In this study, 1'-*O*-methyl-averantin isolated from *Jackrogersella* sp. EL001672 by followed bioactivity-guided fractionation method. *Jackrogersella* sp. EL001672 and 1'-*O*-methyl-averantin suppresses the cancer stemness markers such as ALDH1, CD44, CD133, Lgr-5, Msi-1 and EphB1. In particular, we focused on the SHH signaling pathway that regulates cancer stem cells. Our results showed that crude extract and 1'-*O*-methyl-averantin had inhibitory activity on SHH signaling pathway regulators Gli1, Gli2 and SMO. Furthermore, we identified that 1'-*O*-methyl-averantin regulates the SHH signaling pathway by targeting the Gli1 downstream effector independently of SMO. Finally, we demonstrated the inhibition of the crude extract and 1'-*O*-methyl-averantin on the upstream receptor NOTCH and the downstream effector Hes-1 and the CSL complex. Taken together, the data suggest that 1'-*O*-methyl-averantin isolated from endolichenic fungi suppresses development of CSC by inhibiting the SHH signaling pathway, making it a candidate novel therapeutic agent.

Data availability

All data generated or analysed during this study are included in this published article. All authors read and approved the final manuscript.

Received: 15 September 2022; Accepted: 24 January 2023

Published online: 16 February 2023

References

- Holahan, C., Van Schaeybroeck, S., Longley, D. B. & Johnston, P. G. Cancer drug resistance: An evolving paradigm. *Nat. Rev. Cancer* **13**(10), 714–726 (2013).
- Mertins, S. D. Cancer stem cells: A systems biology view of their role in prognosis and therapy. *Anticancer Drugs* **25**, 353 (2014).
- Yang, Y. *et al.* Tumidulin, a lichen secondary metabolite, decreases the stemness potential of colorectal cancer cells. *Molecules* **23**, 2968 (2018).
- Longley, D. B. & Johnston, P. G. Molecular mechanisms of drug resistance. *J. Pathol.* **205**, 275–292 (2005).
- Karsten, U. & Goletz, S. What makes cancer stem cell markers different?. *Springerplus* **2**, 1–8 (2013).
- Dean, M., Fojo, T. & Bates, S. Tumour stem cells and drug resistance. *Nat. Rev. Cancer* **5**(4), 275–284 (2005).
- Siegel, R. L., Miller, K. D. & Jemal, A. Cancer statistics, 2020. *CA Cancer J. Clin.* **70**, 7–30 (2020).
- Cho, Y. C. *et al.* Bromopropane compounds increase the stemness of colorectal cancer cells. *Int. J. Mol. Sci.* **18**, 1888 (2017).
- Holah, N. S., Aiad, H. A. E. S., Asaad, N. Y., Elkhoully, E. A. & Lasheen, A. G. Evaluation of the role of ALDH1 as cancer stem cell marker in colorectal carcinoma: An immunohistochemical study. *J. Clin. Diagn. Res.* **11**, EC17 (2017).
- Chiou, G. Y. *et al.* Musashi-1 promotes a cancer stem cell lineage and chemoresistance in colorectal cancer cells. *Sci. Rep.* **7**(1), 1–13 (2017).
- Kusano, K. F. *et al.* Sonic Hedgehog myocardial gene therapy: Tissue repair through transient reconstitution of embryonic signaling. *Nat. Med.* **11**(11), 1197–1204 (2005).
- Chen, J. *et al.* Garcinone C suppresses colon tumorigenesis through the Gli1-dependent Hedgehog signaling pathway. *Phytomedicine* **79**, 153334 (2020).
- Sun, Q. *et al.* Berberine suppresses colorectal cancer by regulation of Hedgehog signaling pathway activity and gut microbiota. *Phytomedicine* **103**, 154227 (2022).
- Magistri, P. *et al.* SMO inhibition modulates cellular plasticity and invasiveness in colorectal cancer. *Front. Pharmacol.* **8**, 956 (2018).
- Wu, F., Zhang, Y., Sun, B., McMahon, A. P. & Wang, Y. Hedgehog signaling: From basic biology to cancer therapy. *Cell Chem. Biol.* **24**, 252–280 (2017).
- Guan, Y. *et al.* Kaempferol inhibits renal fibrosis by suppression of the sonic Hedgehog signaling pathway. *Phytomedicine* <https://doi.org/10.1016/J.PHYMED.2022.154246> (2022).
- Zhou, X. *et al.* Rosmarinic acid decreases the malignancy of pancreatic cancer through inhibiting Gli1 signaling. *Phytomedicine* **95**, 153861 (2022).
- Dontu, G. *et al.* Role of Notch signaling in cell-fate determination of human mammary stem/progenitor cells. *Breast Cancer Res.* **6**, 1–11 (2004).

19. Androutsellis-Theotokis, A. *et al.* Notch signalling regulates stem cell numbers in vitro and in vivo. *Nature* **442**(7104), 823–826 (2006).
20. Takebe, N. *et al.* Targeting Notch, Hedgehog, and Wnt pathways in cancer stem cells: Clinical update. *Nat. Rev. Clin. Oncol.* **12**(8), 445–464 (2015).
21. Molnár, K. & Farkas, E. Current results on biological activities of lichen secondary metabolites: A review. *Zeitschrift für Naturforschung Sect. C J. Biosci.* **65**, 157–173 (2010).
22. Tas, I. *et al.* Biological evaluation and phytochemical profiling of some lichen species. *Acta Aliment* **48**, 457–465 (2019).
23. Taş, İ *et al.* Physciosporin suppresses the proliferation, motility and tumorigenesis of colorectal cancer cells. *Phytomedicine* **56**, 10–20 (2019).
24. Yang, Y. *et al.* Potassium usnate, a water-soluble usnic acid salt, shows enhanced bioavailability and inhibits invasion and metastasis in colorectal cancer. *Sci. Rep.* **8**, 1–11 (2018).
25. Yang, Y. *et al.* Acetonic extracts of the endolichenic fungus EL002332 isolated from *Endocarpon pusillum* exhibits anticancer activity in human gastric cancer cells. *Phytomedicine* **40**, 106–115 (2018).
26. Zhou, R. *et al.* The lichen secondary metabolite atranorin suppresses lung cancer cell motility and tumorigenesis. *Sci. Rep.* **7**, 1–13 (2017).
27. Yoo, K. H. *et al.* Transcriptome analysis upon potassium usnate exposure reveals ATF3-induced apoptosis in human gastric and colon cancer cells. *Phytomedicine* **91**, 153655 (2021).
28. Li, X. B. *et al.* Identification and biological evaluation of secondary metabolites from the endolichenic fungus *Aspergillus versicolor*. *Chem. Biodivers.* **12**, 575–592 (2015).
29. He, J. W. *et al.* Heptaketides with antiviral activity from three endolichenic fungal strains *Nigrospora* sp., *Alternaria* sp. and *Phialophora* sp. *Fitoterapia* **83**, 1087–1091 (2012).
30. Jiao, Y. *et al.* New metabolites from endolichenic fungus *Pleosporeales* sp. *Chem. Biodivers.* **12**, 1095–1104 (2015).
31. Li, G. *et al.* Phaeosphaerins A-F, cytotoxic perylenequinones from an endolichenic fungus, *Phaeosphaeria* sp. *J. Nat. Prod.* **75**, 142–147 (2012).
32. Varli, M. *et al.* An acetonic extract and secondary metabolites from the endolichenic fungus *Nemania* sp. EL006872 exhibit immune checkpoint inhibitory activity in lung cancer cell. *Front. Pharmacol.* **0**, 3496 (2022).
33. Li, J. L. *et al.* Antibacterial anthraquinone dimers from marine derived fungus *Aspergillus* sp. *Fitoterapia* **133**, 1–4 (2019).
34. Huang, H. *et al.* Halogenated anthraquinones from the marine-derived fungus *Aspergillus* sp. SCSIO F063. *J. Nat. Prod.* **75**, 1346–1352 (2012).
35. Liang, X. *et al.* Mycotoxins as inhibitors of protein tyrosine phosphatases from the deep-sea-derived fungus *Aspergillus puniceus* SCSIO z021. *Bioorg. Chem.* **107**, 104571 (2021).
36. Pettitprez, A. *et al.* Acquired irinotecan resistance is accompanied by stable modifications of cell cycle dynamics independent of MSI status. *Int. J. Oncol.* **42**, 1644–1653 (2013).
37. Trainer, D. L. *et al.* Biological characterization and oncogene expression in human colorectal carcinoma cell lines. *Int. J. Cancer* **41**, 287–296 (1988).
38. Li, Y., Hibbs, M. A., Gard, A. L., Shylo, N. A. & Yun, K. Genome-wide analysis of N1ICD/RBPJ targets in vivo reveals direct transcriptional regulation of Wnt, SHH, and Hippo pathway effectors by Notch1. *Stem Cells* **30**, 741–752 (2012).
39. Kosanić, M., Manojlović, N., Janković, S., Stanojković, T. & Ranković, B. *Evernia prunastri* and *Pseudovernia furfuraceae* lichens and their major metabolites as antioxidant, antimicrobial and anticancer agents. *Food Chem. Toxicol.* **53**, 112–118 (2013).
40. Lee, S. *et al.* Neuroprotective and anti-inflammatory effects of evernic acid in an MPTP-induced Parkinson's disease model. *Int. J. Mol. Sci.* **22**, 2098 (2021).
41. Solárová, Z. *et al.* Anticancer potential of Lichens' secondary metabolites. *Biomolecules* **10**, 87 (2020).
42. Kim, K. K. & Hur, J. S. Anticancer activity of lichen metabolites and their mechanisms at the molecular level. *Recent Adv. Lichenol. Mod. Methods Approaches Lichen Syst. Cult. Tech.* **2**, 201–208. https://doi.org/10.1007/978-81-322-2235-4_11/COVER (2015).
43. Xu, J. Biomolecules produced by mangrove-associated microbes. *Curr. Med. Chem.* **18**, 5224–5266 (2011).
44. Fouillaud, M., Venkatachalam, M., Girard-Valenciennes, E., Caro, Y. & Dufossé, L. Anthraquinones and derivatives from marine-derived fungi: Structural diversity and selected biological activities. *Mar. Drugs* **14**, 64 (2016).
45. Zhang, J. Y. *et al.* Anthracenedione derivatives as anticancer agents isolated from secondary metabolites of the mangrove endophytic fungi. *Mar. Drugs* **8**, 1469–1481 (2010).
46. Xie, G. *et al.* SZ-685C, a marine anthraquinone, is a potent inducer of apoptosis with anticancer activity by suppression of the Akt/FOXO pathway. *Br. J. Pharmacol.* **159**, 689–697 (2010).
47. Wang, C. C. C., Chiang, Y. M., Kuo, P. L., Chang, J. K. & Hsu, Y. L. Norsolorinic acid from *Aspergillus nidulans* inhibits the proliferation of human breast adenocarcinoma MCF-7 cells via Fas-mediated pathway. *Basic Clin. Pharmacol. Toxicol.* **102**, 491–497 (2008).
48. Ren, H. & Liu, W. W. Nidurufin as a new cell cycle inhibitor from marine-derived fungus *Penicillium flavidorsum* SHK1–27. *Arch. Pharm. Res.* **34**, 901–905 (2011).
49. Wei, W. T., Lin, S. Z., Liu, D. L. & Wang, Z. H. The distinct mechanisms of the antitumor activity of emodin in different types of cancer (review). *Oncol. Rep.* **30**, 2555–2562 (2013).
50. Tumorigenic CancerStemCells, Methods of Isolating and Using the Same. (2011).
51. Gamage, C. D. B. *et al.* Deoxydopodophyllotoxin exerts anti-cancer effects on colorectal cancer cells through induction of apoptosis and suppression of tumorigenesis. *Int. J. Mol. Sci.* **20**, 2612 (2019).
52. Kreso, A. & Dick, J. E. Evolution of the cancer stem cell model. *Cell Stem Cell* **14**, 275–291 (2014).
53. Dai, Y. *et al.* Modified Shenlingbaizhu Decoction represses the pluripotency of colorectal cancer stem cells by inhibiting TGF- β mediated EMT program. *Phytomedicine* **103**, 154234 (2022).
54. Wu, C., Zhu, X., Liu, W., Ruan, T. & Tao, K. Hedgehog signaling pathway in colorectal cancer: Function, mechanism, and therapy. *Onco Targets Ther.* **10**, 3249 (2017).
55. Yang, Y., Nguyen, T. T., Pereira, I., Hur, J. S. & Kim, H. Lichen secondary metabolite physciosporin decreases the stemness potential of colorectal cancer cells. *Biomolecules* **9**, 797 (2019).
56. Watt, F. M. Unexpected Hedgehog-Wnt interactions in epithelial differentiation. *Trends Mol. Med.* **10**, 577–580 (2004).
57. Lu, Y., Li, J., Cheng, J. & Lubahn, D. B. Genes targeted by the Hedgehog-signaling pathway can be regulated by estrogen related receptor β . *BMC Mol. Biol.* **16**, 19 (2015).
58. Moon, J. H. *et al.* Reprogramming fibroblasts into induced pluripotent stem cells with Bmi1. *Cell Res.* **21**(9), 1305–1315 (2011).
59. Muylers-Chen, I. *et al.* Emerging roles of polycomb silencing in X-inactivation and stem cell maintenance. *Cold Spring Harb. Symp. Quant. Biol.* **69**, 319–326 (2004).
60. Gopinath, S. *et al.* Cathepsin B and uPAR regulate self-renewal of glioma-initiating cells through GLI-regulated Sox2 and Bmi1 expression. *Carcinogenesis* **34**, 550–559 (2013).
61. Habib, J. G. & O'Shaughnessy, J. A. The Hedgehog pathway in triple-negative breast cancer. *Cancer Med.* **5**, 2989–3006 (2016).
62. Wu, J. *et al.* The crosstalk between the Notch, Wnt, and SHH signaling pathways in regulating the proliferation and regeneration of sensory progenitor cells in the mouse cochlea. *Cell Tissue Res.* **386**, 281–296 (2021).
63. Ma, X., Drannik, A., Jiang, F., Peterson, R. & Turnbull, J. Crosstalk between Notch and Sonic Hedgehog signaling in a mouse model of amyotrophic lateral sclerosis. *NeuroReport* **28**, 141 (2017).

64. Patni, A. P. *et al.* Comprehending the crosstalk between Notch, Wnt and Hedgehog signaling pathways in oral squamous cell carcinoma—Clinical implications. *Cellular Oncol.* **44**(3), 473–494 (2021).
65. Takebe, N., Harris, P. J., Warren, R. Q. & Ivy, S. P. Targeting cancer stem cells by inhibiting Wnt, Notch, and Hedgehog pathways. *Nat. Rev. Clin. Oncol.* **8**(2), 97–106 (2010).
66. McAuliffe, S. M. *et al.* Targeting Notch, a key pathway for ovarian cancer stem cells, sensitizes tumors to platinum therapy. *Proc. Natl. Acad. Sci. USA* **109**, E2939–E2948 (2012).
67. Jin, Y. H. *et al.* Beta-catenin modulates the level and transcriptional activity of Notch1/NICD through its direct interaction. *Biochim. Biophys. Acta Mol. Cell Res.* **1793**, 290–299 (2009).
68. Visvader, J. E. & Lindeman, G. J. Cancer stem cells: Current status and evolving complexities. *Cell Stem Cell* **10**, 717–728 (2012).
69. Visioli, A. *et al.* Stemness underpinning all steps of human colorectal cancer defines the core of effective therapeutic strategies. *EBioMedicine* **44**, 346–360 (2019).
70. Haraguchi, N. *et al.* CD133+CD44+ population efficiently enriches colon cancer initiating cells. *Ann. Surg. Oncol.* **15**, 2927–2933 (2008).
71. Todaro, M., Francipane, M. G., Medema, J. P. & Stassi, G. Colon cancer stem cells: Promise of targeted therapy. *Gastroenterology* **138**, 2151–2162 (2010).
72. Liu, Y. S., Hsu, H. C., Tseng, K. C., Chen, H. C. & Chen, S. J. Lgr5 promotes cancer stemness and confers chemoresistance through ABCB1 in colorectal cancer. *Biomed. Pharmacother.* **67**, 791–799 (2013).
73. Kemper, K. *et al.* Monoclonal antibodies against Lgr5 identify human colorectal cancer stem cells. *Stem Cells* **30**, 2378–2386 (2012).
74. Holmberg, J. *et al.* EphB receptors coordinate migration and proliferation in the intestinal stem cell niche. *Cell* **125**, 1151–1163 (2006).
75. Grandi, A. *et al.* Targeting the Eph/ephrin system as anti-inflammatory strategy in IBD. *Front. Pharmacol.* **10**, 691 (2019).
76. Papadakos, S. P., Petrogiannopoulos, L., Pergaris, A. & Theocharis, S. The EPH/ephrin system in colorectal cancer. *Int. J. Mol. Sci.* **23**, 2761 (2022).
77. Ginestier, C. *et al.* ALDH1 is a marker of normal and malignant human mammary stem cells and a predictor of poor clinical outcome. *Cell Stem Cell* **1**, 555–567 (2007).
78. Van Der Waals, L. M., Rinkes, I. H. M. B. & Kranenburg, O. ALDH1A1 expression is associated with poor differentiation, ‘right-sidedness’ and poor survival in human colorectal cancer. *PLoS ONE* **13**, e0205536 (2018).
79. Bao, C. *et al.* Amentoflavone inhibits tumorsphere formation by regulating the Hedgehog/Gli1 signaling pathway in SUM159 breast cancer stem cells. *J. Funct. Foods* **61**, 103501 (2019).
80. Bora-Singhal, N., Perumal, D., Nguyen, J. & Chellappan, S. Gli1-mediated regulation of Sox2 facilitates self-renewal of stem-like cells and confers resistance to EGFR inhibitors in non-small cell lung cancer. *Neoplasia* **17**, 538–551 (2015).
81. Gonnissen, A. *et al.* Targeting the Hedgehog signaling pathway in cancer: Beyond smoothed. *Oncotarget* **6**, 13899–13913 (2015).
82. Zhao, D. *et al.* NOTCH-induced aldehyde dehydrogenase 1A1 deacetylation promotes breast cancer stem cells. *J. Clin. Investig.* **124**, 5453–5465 (2014).
83. Mu, X., Isaac, C., Greco, N., Huard, J. & Weiss, K. Notch signaling is associated with ALDH activity and an aggressive metastatic phenotype in murine osteosarcoma cells. *Front. Oncol.* **3**, 143 (2013).
84. Sullivan, J. P. *et al.* Aldehyde dehydrogenase activity selects for lung adenocarcinoma stem cells dependent on notch signaling. *Cancer Res.* **70**, 9937–9948 (2010).
85. Singh, S. *et al.* ALDH1B1 is crucial for colon tumorigenesis by modulating Wnt/ β -catenin, Notch and PI3K/Akt signaling pathways. *PLoS ONE* **10**, e0121648 (2015).
86. Santini, R. *et al.* Hedgehog-Gli signaling drives self-renewal and tumorigenicity of human melanoma-initiating cells. *Stem Cells* **30**, 1808–1818 (2012).
87. Geyer, N. & Gerling, M. Hedgehog signaling in colorectal cancer: All in the stroma?. *Int. J. Mol. Sci.* **22**, 1025 (2021).
88. Raz, G. *et al.* Hedgehog signaling pathway molecules and ALDH1A1 expression in early-stage non-small cell lung cancer. *Lung Cancer* **76**, 191–196 (2012).
89. Charles Gorst-Allman, B. P. *et al.* Carbon-13 nuclear magnetic resonance assignments of some fungal C 20 anthraquinones; their biosynthesis in relation to that of aflatoxin B 1. *J. Chem. Soc. Perkin* **1**(0), 2181–2188 (1977).
90. Wu, C. J., Li, C. W. & Cui, C. B. Seven new and two known lipopeptides as well as five known polyketides: The activated production of silent metabolites in a marine-derived fungus by chemical mutagenesis strategy using diethyl sulphate. *Mar. Drugs* **12**, 1815–1838 (2014).
91. Guo, L. D. *et al.* Molecular identification of white morphotype strains of endophytic fungi from *Pinus tabulaeformis*. *Mycol. Res.* **107**, 680–688 (2003).
92. Gardes, M. & Bruns, T. D. ITS primers with enhanced specificity for basidiomycetes—Application to the identification of mycorrhizae and rusts. *Mol. Ecol.* **2**, 113–118 (1993).
93. Vilgalys, R. & Hester, M. Rapid genetic identification and mapping of enzymatically amplified ribosomal DNA from several *Cryptococcus* species. *J. Bacteriol.* **172**, 4238–4246 (1990).
94. Taş, İ *et al.* Inflammatory and tumorigenic effects of environmental pollutants found in particulate matter on lung epithelial cells. *Toxicol. In Vitro* **59**, 300–311 (2019).
95. Microplate Software: BioTek Gen5 Data Analysis Software—Overview. <https://www.biotek.com/products/software-robotics-software/gen5-microplate-reader-and-imager-software/overview/>.
96. Zhou, R., Nguyen, T. T., Kim, K. K., Hur, J.-S. & Kim, H. Extracts from lichen *Lobaria retigera* decrease the stemness potential of colorectal cancer cells. *Mater. Express* **12**, 234–240 (2022).
97. IMT—Image & Microscope Technology—Image analysis software developer. <http://www.imt-digital.com/english/html/productsIMT.php>.
98. Park, S. Y. *et al.* KITENIN-targeting MicroRNA-124 suppresses colorectal cancer cell motility and tumorigenesis. *Mol. Ther.* **22**, 1653–1664 (2014).
99. Le, T. C. *et al.* Marine depsipeptide nobilamide I inhibits cancer cell motility and tumorigenicity via suppressing epithelial-mesenchymal transition and MMP2/9 expression. *ACS Omega* **7**, 1722–1732 (2022).
100. CFX Connect™ Real-Time PCR Detection System Addendum to CFX96 Touch™ and CFX384 Touch™ Real-Time PCR Detection Systems Instruction Manual Catalog #185-5200.
101. SigmaPlot—Inpixon—systatsoftware.com. <https://systatsoftware.com/sigmaplot/>.

Acknowledgements

This work was supported by the National Research Foundation of Korea grant (NRF-2020R1C1C1007832) funded by the Korea government (MSIP).

Author contributions

M.V. and H.K. conceived and designed the experiments. M.V., Y.Y., R.Z., Í.T., S.P., C.G., and S.-Y.P. performed the biological experiments. E.-Y.L., and S.-J.N. performed the bioactivity-guided fractionation of a crude extract and identified the single compounds. J.-S.H. contributed materials. M.V. and H.K. analyzed the data and wrote the manuscript.

Competing interests

The authors declare no competing interests.

Additional information

Supplementary Information The online version contains supplementary material available at <https://doi.org/10.1038/s41598-023-28773-z>.

Correspondence and requests for materials should be addressed to S.-J.N. or H.K.

Reprints and permissions information is available at www.nature.com/reprints.

Publisher's note Springer Nature remains neutral with regard to jurisdictional claims in published maps and institutional affiliations.



Open Access This article is licensed under a Creative Commons Attribution 4.0 International License, which permits use, sharing, adaptation, distribution and reproduction in any medium or format, as long as you give appropriate credit to the original author(s) and the source, provide a link to the Creative Commons licence, and indicate if changes were made. The images or other third party material in this article are included in the article's Creative Commons licence, unless indicated otherwise in a credit line to the material. If material is not included in the article's Creative Commons licence and your intended use is not permitted by statutory regulation or exceeds the permitted use, you will need to obtain permission directly from the copyright holder. To view a copy of this licence, visit <http://creativecommons.org/licenses/by/4.0/>.

© The Author(s) 2023